

ABAQUS FEM ANALYSIS OF THE POSTBUCKLING BEHAVIOUR OF COMPOSITE SHELL STRUCTURES

T. Möcker¹, P. Linde³, S. Kraschin², F. Goetz¹, J. Marsolek¹, W. Wohlers³

¹ Abaqus Deutschland GmbH, 52062 Aachen, Germany, E-mail: Torsten.MOECKER@3ds.com

² Bishop GmbH - Aeronautical Engineers, 22587 Hamburg, Germany

³ Airbus Deutschland GmbH, 21129 Hamburg, Germany

Keywords: postbuckling, FEM, crippling, failure load, damage model, fastener, cohesive behaviour

Abstract

For the design of stiffened composite shell structures the knowledge of the structural response in the postbuckling region is an important topic. Accordingly, tools are required that enable an accurate and reliable prediction of the postbuckling behaviour. In this paper it is shown how the finite element code Abaqus can be used for this purpose. When performing finite element simulations, a large amount of time is often needed to build up the finite element model - in particular if the model consists of several parts with complex geometries. For this reason the preprocessing tool Abaqus/CAE provides an interface which allows the user to automate repetitive tasks. Based on this interface, a tool simplifying the pre- and postprocessing of shell structures stiffened by stringers and frames was developed by Abaqus Deutschland for the company Airbus. Next to a summary of the abilities of this tool, the main focus of this paper is on discussing several modelling techniques that are used to enable a realistic idealisation of the physical problem and on presenting simulation results for an exemplary structure. Based on this example, the influence of modelling details like mesh density and geometric imperfections on the prediction of the failure load is discussed.

1 Generating the Finite Element Model

In the design and development of aircraft fuselage structures, both theoretical analyses and experimental tests of the static behaviour play important roles in certification and technology processes. In particular, stiffened fuselage panels have to be analysed with respect to their buckling and postbuckling behaviour. Theoretical predictions have to be validated by a substantial number of experimental tests which are both expensive and utterly time consuming.

To reduce the number of physical tests, finite element simulations of the test rig are carried out at the company Airbus with the code Abaqus. Since a large number of finite element models with similar geometries have to be built up, a graphical user interface (called SIMULPAC¹ - **S**imulation of **P**anels in **A**ircrafts) was developed using the core functionality of Abaqus/CAE. The programming language behind SIMULPAC is Python. SIMULPAC provides an automated design environment for the modelling and simulation of aircraft panels with different boundary conditions, e.g. with shear-compression test-rig conditions.

The basic concept of SIMULPAC is to provide the user with all tools required to create a finite element model of a stiffened panel based on the parametric modelling principles of Abaqus/CAE in order to reduce the time for model generation significantly compared to the usual manual preprocessing. To achieve this goal, SIMULPAC extends the graphical user interface of Abaqus/CAE. E.g. a new model tree is added to the model and results tree already existing in Abaqus/CAE. This new tree guides the user through all steps required to generate the model of a stiffened aircraft panel (e.g. generation of stringers, frames, clips; definition of connectivity between structural parts). Within all of these steps, the user has to define the corresponding geometry based on predefined parameters which can be modified later on. Once the user has provided all of the required data, SIMULPAC generates the finite element model automatically. The final, generated model of a shear-compression test rig panel is shown in Figure 1. Subsequently, the user can add further features to the finite element model, which are not yet supported by SIMULPAC.

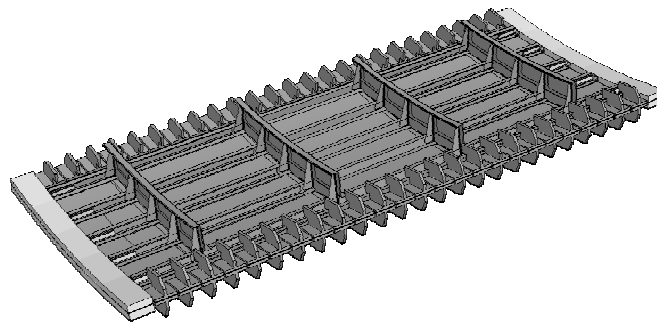


Fig. 1 Model of shear-compression test rig panel generated by SIMULPAC

2 Details of the Finite Element Model

The models generated by SIMULPAC include a lot of individual modelling techniques enabling a realistic representation of the physical problem. Only some selected, basic techniques are discussed in this chapter, since not all details of the finite element model can be given in this abstract. The following description is not limited to the features used for the simulations presented in chapter 3, but also includes further information, which is important for other analyses.

2.1 Material models for composite structures

In the finite element models created by SIMULPAC all structural components (skin, stringers, frames, clips) are idealised by shell elements. There are no restrictions on the material models to be used for the different parts of the structure. Either homogeneous or composite (layered) shell sections can be assigned to the elements. Composite shell sections are appropriate to define a lay-up consisting out of an arbitrary number of individual layers with isotropic or orthotropic material properties.

For UD laminates the orthotropic response of the undamaged material is assumed to be linearly elastic. If damage has to be taken into account, it can occur due to four different failure modes: fibre rupture in tension, fibre buckling or kinking in compression, matrix cracking under transverse tension and shearing and matrix crushing under transverse compression and shearing. To predict the initiation of failure due to one of these failure modes, different failure criteria are known (e.g. Hashin³, Puck⁴). The failure criteria can be either evaluated during postprocessing or can be used for more sophisticated damage models enabling a simulation of the stiffness and strength reduction due to material damage processes. Abaqus provides such a damage model based on the Hashin criteria. However, user subroutine interfaces are available for the programming of user-defined damage models, which may be based on other criteria. At Airbus appropriate damage models are currently under development.

2.2 Modelling of riveted and bonded connections

Important manufacturing techniques to connect different parts of stiffened shell structures to each other, e.g. to connect the stringers to the skin, are riveting and bonding. How these two types of connections can be idealised in a finite element model generated by SIMULPAC is discussed in this section.

An appropriate way for representing rivets in an Abaqus model is the use of fasteners. Fasteners provide a kinematic connection between two nodes. These nodes are attached to the surfaces which have to be connected. As the fastener capability is mesh-independent, the attachment is realised by coupling constraints, i.e. the end nodes of the fasteners are connected to the surrounding nodes on the surfaces by a constraint equation.

Different properties can be assigned to the six degrees of freedom which define the structural behaviour of the fastener. In the finite element models discussed in this paper, the riveted connection is idealised by assuming that the rotation about the rivet axis is free, that the two bending rotations are suppressed and that the behaviour in the three translational directions (axial and shear directions) is linear elastic. In general, the behaviour assigned to the fasteners can be more complex, features like plasticity or damage models can be added.

To idealise bonded connections, several techniques are available in Abaqus. The easiest way is to use a tie constraint between the surfaces to be connected. A tie constraint is mesh-independent and connects the surfaces rigidly to each other throughout the whole analysis. Since Abaqus version 6.8, a new contact functionality is available, which allows the surfaces to be connected using a cohesive behaviour at the interfaces. The cohesive behaviour can include linear elastic properties and, if required, a fracture energy based damage model similar to the one available for the damage of fibre-reinforced composites. This new functionality is an alternative to the use of cohesive elements at the interface and enables the simulation of debonding or delamination processes. Furthermore, a user subroutine interface UINTER is provided for the definition of user-defined interface behaviours.

2.3 Modelling of strain gauges

In order to provide data which is directly comparable to test results, an idealisation of strain gauges is included in SIMULPAC. For this purpose, axial connectors are used, which enable the connection of two nodes without any additional stiffness. To model the strain gauges, two reference points are defined on the top or bottom surface of the skin. The distance between the reference points corresponds with the length of the strain gauges used in the tests. Both reference points are connected either to the top or to the bottom surface of the skin by a tie constraint (*TIE²).

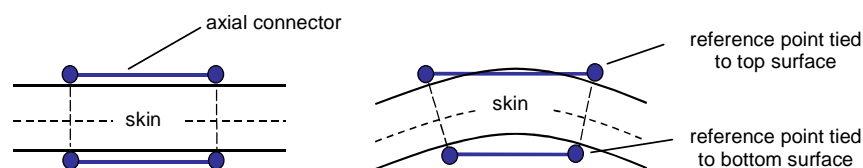


Fig. 2 Idealization of strain gauges, undeformed (left) and deformed (right) configuration

An axial connector is defined between these reference points. The advantage of this modelling technique is that the relative displacement between the reference nodes in the axial direction of the connector is directly available for output and can be used to determine the strain by dividing the relative displacement by the connector length. Figure 2 illustrates how strain gauges on the top and the bottom of the skin can be idealised in this way. Both, single-channel strain gauges and triple-channel strain gauges (rosettes) can be defined.

3 Comparison of Simulation and Test Results

To demonstrate the applicability of the methods described above for predicting the postbuckling and failure behaviour of stiffened shell structures, simulation results of an exemplary structure are presented and compared to test results. In addition, the influence of modelling aspects like mesh density and imperfections is discussed.

3.1 Geometry of the test structure and expected type of failure

The structure which is used as an example in this paper was tested at Airbus, and the finite element model was created by the tool SIMULPAC described in chapters 1 and 2. Figure 1 shows the geometry of this test panel. It contains five Z-type stringers and four Z-type frames, which are connected to the skin and to the stringers by clips. The skin is made out of Glare, a laminate containing aluminium and glass fibre reinforced layers. Both, the stringers and the clips are connected to the adjacent parts by rivets. In the finite element model this type of connection is realised by a small sliding contact formulation and by the use of fasteners as described in section 2.2. A combination of axial compression and shear loads is applied to the panel along the outer edges.

The design of the panel takes into account that the structural behaviour in the centre of the panel is of interest. Accordingly, the outer areas of the panel are reinforced to ensure that the panel does not fail close to the load introduction areas. As expected, failure was observed in the test and in the simulation in between the two inner frames. Figure 3 shows that this panel failed due to forced crippling. This type of failure is a local failure of the stringers initiated by the bending deformation, which results from the shear buckles at the bottom of the stringer. In the test failure occurred at 1.72 times limit load (LL).

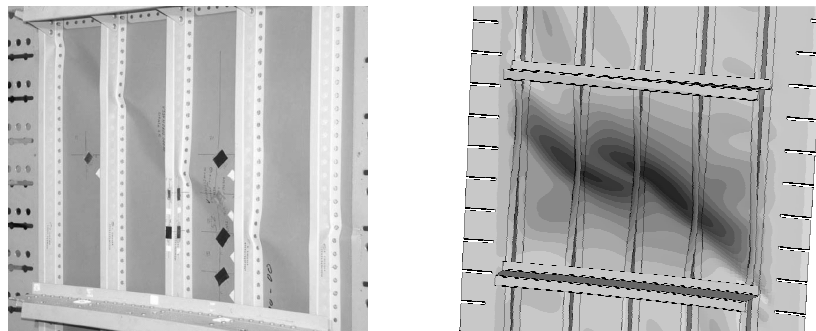


Fig. 3 Forced crippling failure in the centre of the panel (test and finite element prediction)

3.2 Influence of mesh density and imperfections

This test was simulated with two different Abaqus models: one with a coarse mesh for the stringers (element edge length: approx. 10mm) and one with a fine mesh on the stringers (element edge length: approx. 3mm). The meshes on the other structural parts are identical in both simulations. There are no significant differences between both simulations when comparing the skin buckling load, the buckling pattern and the initial postbuckling behaviour. E.g. the buckling pattern directly after buckling onset is shown for both simulations in Figures 4 and 5.

However, there is a significant influence of the stringer mesh density on the collapse load. The simulation with a coarse stringer mesh predicts a failure load of 2.04 LL, while the failure load predicted by the simulation with a fine stringer mesh is 1.78 LL. Obviously, this difference is caused by the type of failure to be predicted. The local bending deformation of the stringers due to the shear buckles leads to local stress peaks in the stringers. To calculate these stress peaks accurately, a refined stringer mesh is required. In Figures 4 and 5 the distribution of the output variable PEEQ (equivalent plastic strain) is plotted for both stringer meshes at the same load level (1.7 LL). The stringer region shown in these figures refers to the area where failure occurs. For the fine mesh the peak of the equivalent plastic strain is higher compared to the results for the coarse mesh by a factor of 5 to 10. Accordingly, the failure load determined with the fine mesh is smaller and is quite close to the experimental result.

The results presented so far refer to simulations with reduced integration shell elements (S4R elements). In addition, the analysis with the refined stringer mesh was repeated with fully integrated shell elements (S4 elements). The results obtained are nearly identical to those obtained with S4R elements except for the failure load. With S4R elements the failure load is 1.78 LL, which is close to the experimental value, while the simulation with S4 elements gives 1.90 LL. When comparing the results in more detail, it becomes obvious that the reason for this difference is the direction of the

skin buckling pattern. With S4 elements the direction of the buckling pattern is opposite to the one obtained with S4R elements, even though the shape is the same. Due to the different buckling direction a slightly different deformation pattern at collapse develops in the analysis with S4 elements, which causes an increased collapse load compared to the analysis with S4R elements and the inverse buckling direction.

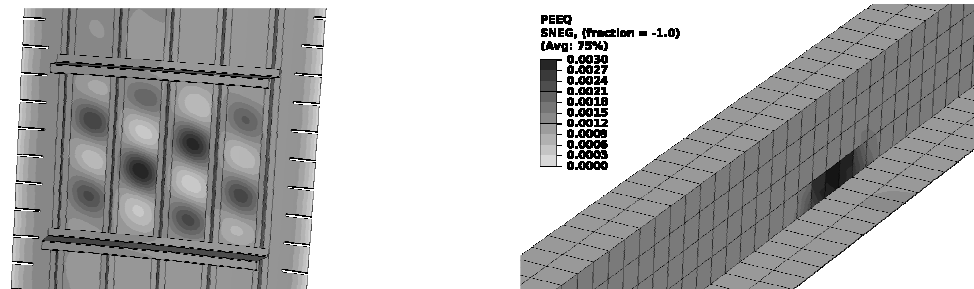


Fig. 4 Buckling pattern at 0.52 LL and distribution of PEEQ in stringer at 1.7 LL (coarse mesh on stringer)

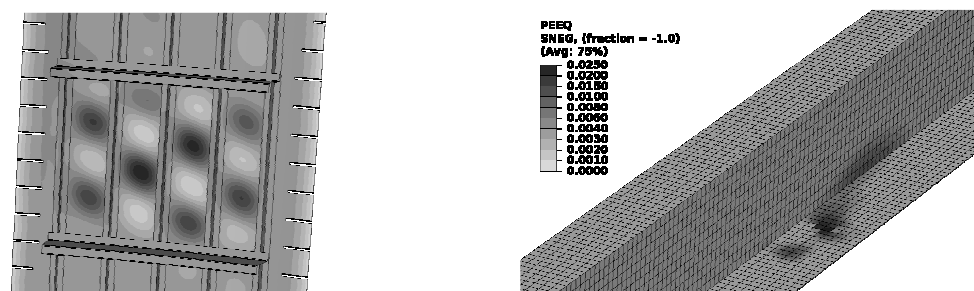


Fig. 5 Buckling pattern at 0.52 LL and distribution of PEEQ in stringer at 1.7 LL (fine mesh on stringer)

In both simulations it was assumed that the panel geometry is perfect. For this reason, the buckling direction, which develops in the nonlinear analysis is arbitrary, and small changes in the numerical formulation of the problem (like choosing a different element type) may cause the buckling direction to change. The only way to prescribe the buckling direction in the numerical model is to use imperfections. In Abaqus this can be done based on the results of a preceding linear buckling analysis by adding the input file option **IMPERFECTION*². To verify that the increase of the collapse load is caused by the change of the buckling direction, the analysis with S4R elements was repeated with an initial imperfection, which enforces the buckling pattern to have the same direction as in the simulation with S4 elements. The maximum imperfection in this model is 0.05mm, which is 2.5% of the skin thickness. This simulation gives a failure load of 1.90 LL which is nearly identical to the result from the simulation with S4 elements.

3.3 Comparison to test results

Most of the results from the finite element analysis show a quite good agreement with the test results. In Figure 3 the experimental deformation pattern at collapse is compared to the numerical result. The skin buckling load, which can be determined from strain gauge measurements, was approx. 0.5 LL in the test and the numerical prediction is 0.44 LL. Furthermore, there is a good agreement in the failure loads in simulation and test (test: 1.72 LL, simulation: 1.78 LL) and in the load displacement curves, which are not shown in this abstract.

References

1. Costamagna, K., Frenk, A., Emmel, T., Virtual Testing of Aircraft Panels, Abaqus Benutzerkonferenz, Baden-Baden, 2007.
2. Dassault Systèmes Simulia Corp., Abaqus Analysis User's Manual, Version 6.8, Providence, RI, USA, 2008.
3. Hashin, Z., Failure Criteria for Unidirectional Fiber Composites, Journal of Applied Mechanics, vol. 47, pp. 329–334, 1980.
4. Puck, A., Festigkeitsanalyse von Faser-Matrix-Laminaten, Carl Hanser Verlag, München, Wien, 1996.